A coarse grained model for granular compaction and relaxation

D. A. Head* and G. J. Rodgers†

Institute of Physical and Environmental Sciences, Brunel University, Uxbridge, Middlesex, UB8 3PH, United Kingdom

(October 30, 2006)

We introduce a theoretical model for the compaction of granular materials by discrete vibrations which is expected to hold when the intensity of vibration is low. The dynamical unit is taken to be clusters of granules that belong to the same collective structure. We rigorously construct the model from first principles and show that numerical solutions compare favourably with a range of experimental results. This includes the logarithmic relaxation towards a statistical steady state, the effect of varying the intensity of vibration resulting in a so-called "annealing" curve, and the power spectrum of density fluctuations in the steady state itself. A mean field version of the model is introduced which shares many features with the exact model and is open to quantitative analysis.

PACS numbers: 05.40.+j. 46.10.+z, 64.60.L, 81.05.Rm, 81.20.Ev

I. INTRODUCTION

Extrapolating bulk properties from the underlying microscopic dynamics is generally more difficult with granular materials than with gases, a difficulty that has been attributed, at least in part, to the lack of thermal averaging [1,2]. Unlike molecules, granules are static at room temperature and so cannot explore phase space without some external impetus. For example, consider a column of loosely packed granules in a cylindrical container, where *loosely packed* means that there are typically large gaps or *voids* between neighbouring granules. It is energetically favourable for the granules to collectively reorganise to a state which minimises these voids, since a more compact column will have a lower centre of gravity and hence a lower potential energy. That this does not occur spontaneously is a direct consequence of the lack of thermal motion. One way to allow the column to evolve is simply to *tap* or otherwise perturb the container, thus giving the granules a small amount of kinetic energy with which to rearrange. This process has been studied empirically in the context of industrial applications [3], but only recently have attempts been made to try to understand the fundamental dynamics involved.

Mehta *et.al.* [4–6] employed a non-sequential Monte Carlo algorithm to simulate the process on a microscopic level. *Non-sequential* means that granules are allowed to move and settle simultaneously, which is important in this context since it allows for the cooperative reorganisation of granule-granule contacts. These simulations predict that granular media should relax on two time scales, corresponding to individual granule motion and collective processes respectively. However, this is not in accord with the experimental work of Knight *et.al.* [7]. They measured the rate of compaction in a column of monodisperse glass beads that was subjected to discrete vertical vibrations. The plot of density against the number of vibrations was found to be best described by $\rho(t) \sim (\log t)^{-1}$, where the time ordinate t is proportional to the number of taps. One possible reason for the discrepancy between the simulations and the experiments may simply be that the regimes of vibration intensity studied were different. The smallest vibration considered in the simulations corresponds to a 5% increase in volume at every tap, which is much more than the experiments involved.

A number of models embracing a variety of theoretical approaches have been introduced to try and account for the experimental findings. Of those we are aware of, one is a phenomenological macroscopic model [8], but the remainder are all microscopic in nature. The slow relaxation has been attributed by Ben-Naim *et.al.* to the large number of reconfigurations required to bring enough small voids together to make one void large enough to absorb another granule [9–11]. de Gennes also chose to focus on the voids and found that a Poisson distribution of void sizes could give rise to the expected inverse logarithmic relaxation [12]. Coglioti *et.al.* have introduced a lattice model in which each granule can be in one of two states with each state corresponding to a different geometrical orientation [13,14]. The motion between neighbouring granules is constrained by their relative orientations, hence the rate of relaxation in their model is governed by a form of *geometrical frustration*.

In this paper, we introduce a model for granular compaction which is neither macroscopic nor microscopic but instead lies somewhere between these two extremes. It is *coarse grained* in that it takes *clusters* of granules as its dynamical unit rather than individual granules. This approach is based on the picture of granular interactions described by Mehta *et.al.* in relation to their simulations [4–6], except that here we are interested in the limit of weak vibrations. The resulting model is strikingly similar to one already devised by Bak and Sneppen in a wildly different context, that of biological evolution [15,16]. In Sec. II the model is described in detail and its physical basis is explained. Careful consideration is given to the range of validity of our assumptions. Results of numerical simulations are compared to the experimental findings in Sec. III. The exact solution of a mean field version of the model is investigated in Sec. IV.

Finally, with give a summary of the model in Sec. V.

II. THE MODEL

Mehta *et.al.* picture the granular media as being subdivided into local clusters, as in Fig. 1(a), where a cluster is defined as a group of granules belonging to the same multi-particle potential well [4–6]. A vibration with an intensity equivalent to the binding energy of a granule to its well causes that granule to be ejected and move independently of the others. Under weaker vibrations, all the granules remain in the well but still reorganise collectively, albeit on a slower time scale to individual particle motion. Although this description seems to be valid for the range of intensities of vibration considered in their simulations, it clearly fails for the much lower intensities relevant to the experiments [7,11]. We believe that the picture is essentially correct but needs to be modified to describe the behaviour of the system deep in the collective relaxation regime. To do this, we first need to closely analyse exactly what is meant by a multi-particle potential well.

Any given configuration of an ensemble of particles can be represented by a single point in the space of all possible configurations. Each allowed configuration has a well defined potential energy, and so the time evolution of the ensemble under gravity can be described by a walk in configuration space over a potential energy *landscape.* Now, the preferred state for each individual granule is simply resting at the bottom of the container. If the granules did not interact, then the ensemble would trivially evolve to the global minimum with every granule in its preferred state, i.e. all resting on the bottom. Of course, real granules do interact, and one granule moving downwards will inevitably push some of the surrounding granules upwards slightly. The ensemble is thus *frustrated* in that it cannot simultaneously satisfy each granule's tendency to move downwards. In terms of the potential energy landscape, this frustration results in a rugged landscape with many local minima separated by barriers of various heights. A schematic example is given in Fig. 2, where for clarity we have compressed the entire configuration space onto a single axis.

The ensemble will be at a local minimum between perturbations. The effect of the perturbation is to move the ensemble to a point higher up on the landscape before it again relaxes, possibly to a different minimum. For the low-energy perturbations we are concerned with here, the ensemble will usually move between nearby minima and consequently only a small number of granules will change their position or orientation. Following Mehta *et.al.* we assume that these granules typically belong to some sort of collective structure, such as an arch or bridge. Thus the system can be subdivided into localised *clusters*, where a cluster is now defined as the *unit of collective reconfiguration.* Furthermore, we map the system onto a lattice in which every site corresponds to a single cluster, as in Fig. 1. This lattice representation is implicitly static and so will not be valid if there is any form of global motion in the system, such as convection or surface flow, although it should still hold if there is only a limited amount of local motion. Large perturbations will involve reorganisation on a system-wide scale and the rapid rearrangement of cluster boundaries, so the lattice representation is again expected to fail in such situations.
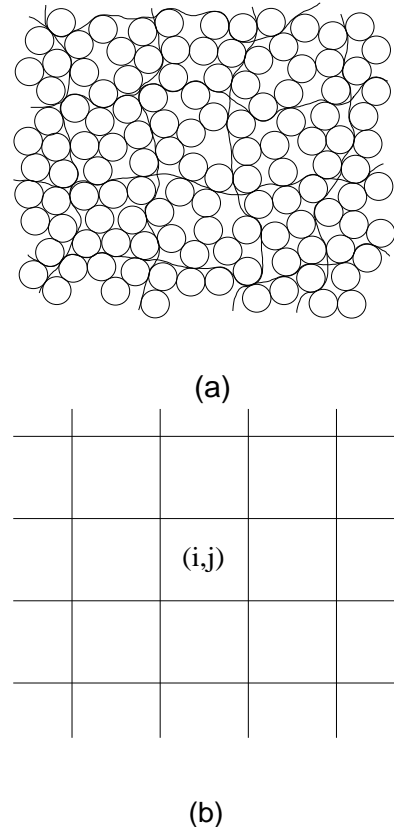

(a)

(b)

FIG. 1. An example of the process of subdividing granular media into local clusters, given here for the case of two dimensions. (a) A collection of circular granules separated into clusters. The thick lines represent boundaries between neighbouring clusters. (b) The corresponding lattice representation. Each site (i, j) denotes a single cluster.

We now have a lattice of clusters, each of which move on their own individual potential energy landscapes. During the perturbation, each cluster is kicked to a point higher up on its landscape, and those that subsequently relax to a new minimum have collectively reconfigured. When a cluster reconfigures the contacts between it and adjacent clusters will be redistributed in a highly non-trivial manner, the pattern of stress lines will be locally distorted and the boundaries between adjacent clusters may shift slightly to accommodate different granules. As a consequence, there will be a significant change in the landscapes of the cluster itself and those near to it. In particular, we note that the heights of barriers between

2

minima will change. It may seem possible for one of the nearby clusters to move a significant distance on its new landscape before finding a minimum, effectively constituting another reconfiguration event. However, this contradicts the definition of a cluster as the fundamental unit of collective reconfiguration, since any two clusters that interact in this way should have been treated as a single cluster in the first place. Thus it can safely be assumed that nearby clusters will not reconfigure, although the heights of barriers in their landscapes will still change.

Significant progress can be made if we do away with the landscapes altogether and just deal with the heights of barriers between minima instead. Indeed, as we are only interested in the limit of weak perturbations, we can go one step further and disregard all but the *smallest* barrier, since this will almost always be the one that is involved anyway. Each reconfiguration is assumed to alter the landscapes in such a complicated manner that, to good approximation, the height of a barrier can be taken to be a random number drawn from a suitable probability distribution. Although this distribution is in general unknowable, we have found the model to be robust to a variety of different choices, including uniform, exponential and Gaussian (*robustness* means that the essential behaviour of the system remains unchanged with respect to the modifications tried). We subsequently use the uniform probability distribution $P(b)$ for barrier height b, where

$$P(b) = \begin{cases} 1 & \text{for } b \in [0,1], \text{ and} \\ 0 & \text{otherwise.} \end{cases} \tag{1}$$

Consider now the effect of the external perturbation on just a single cluster with a barrier height of b_{clust}. Suppose that the effect of the perturbation is for the cluster to gain an energy of e_Γ and to move to a corresponding point higher up on its landscape. If $e_\Gamma < b_{\text{clust}}$, the cluster cannot cross even its lowest barrier and so we can be sure that it will relax to the same minimum that it was at before. However, if $e_\Gamma \geq b_{\text{clust}}$ then there is a non-zero probability that the cluster will reconfigure. We take this probability to be of the form

$$\begin{cases} \propto \exp\left\{-\mu\left(\frac{e_\Gamma}{e_\Gamma - b_{\text{clust}}}\right)\right\} & \text{for } e_\Gamma > b_{\text{clust}}, \\ = 0 & \text{for } e_\Gamma \leq b_{\text{clust}}, \end{cases} \tag{2}$$

where μ is a dimensionless constant. This may appear to be a somewhat arbitrary choice, but a number of variations with a suitable cut-off at $e_\Gamma = b_{\text{clust}}$ were tried, and no essential difference in system behaviour was observed. The choice of (2) was made since it is exponential in form, implying some sort of underlying Poisson process, and it has the correct asymptotics for $e_\Gamma \to b_{\text{clust}}$ and $e_\Gamma \to \infty$.
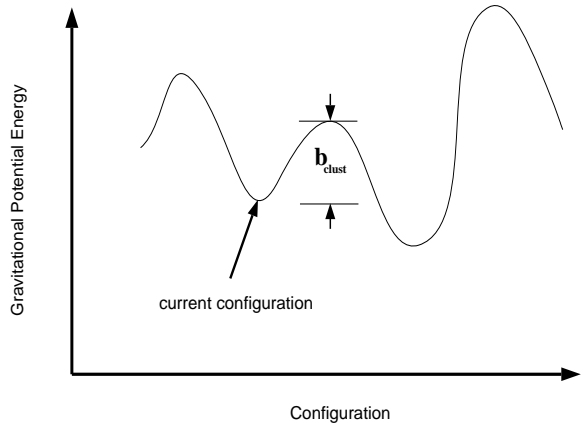

FIG. 2. Schematic example of a potential energy landscape for an ensemble of granules in configuration space. The ensemble currently lies at the local minimum marked. The smallest barrier to an adjacent minimum has a height of b_{clust}.

When the container is vibrated, the associated energy impulse is distributed in some undefined manner to all the clusters in the system. We have observed little qualitative difference arising from distributing this energy stochastically and henceforth assume that each cluster receives the same energy e_Γ. It should be clear from (2) that the cluster with the smallest barrier in the system, say of height b_{min}, is the most likely to reconfigure. With this observation, we can make a further simplification that also makes little difference to the system behaviour, which is to assume that the cluster that reconfigures first is *always* the one with the barrier height of b_{min}. Thus there is no longer any need to simulate every perturbation until the cluster reconfigures, we can instead just reconfigure the cluster immediately and advance the time by an amount δt, where

$$\delta t \propto \exp\left\{\mu\left(\frac{e_\Gamma}{e_\Gamma - b_{\text{min}}}\right)\right\}. \tag{3}$$

This is the expected number of perturbations of energy e_Γ required until the cluster with barrier height b_{min} reconfigures, and is the reciprocal of (2). For $b_{\text{min}} \leq e_\Gamma$, δt is taken to be infinite.

We are now in a position to describe the model algorithmically. The granular media is represented by a lattice, each site of which corresponds to a unit of collective reconfiguration, ie. a cluster. The model is robust to variations in lattice connectivity, so without loss of generality we choose a simple cubic array. Each cluster (i, j, k) has an associated potential energy barrier against reconfiguration, b_{ijk}, drawn from the probability distribution $P(b)$ given in (1). The external perturbation takes the form of an energy impulse distributed uniformly throughout the system, each cluster receiving an amount e_Γ. At each algorithm step, the cluster with the smallest barrier in the system, b_{min}, is found. If $e_\Gamma \leq b_{\text{min}}$ then the perturbation is too weak to cause any reconfiguration events, the system is frozen and the simulation is complete. If $e_\Gamma > b_{\text{min}}$, the cluster in question and the 6 clusters ad-

jacent to it are reconfigured - that is, their barriers are redrawn from the same probability distribution as before. The real time is increased by an amount δt defined in (3), and the simulation moves on to the next algorithm step. Note that we do not employ periodic boundary conditions, instead clusters at the faces, edges or corners of the lattice simply have 5, 4 or 3 adjacent clusters, respectively.

Numerical solutions of the model are presented in the following section. For now, we would like to remark upon the strong similarity between this model and a model of biological evolution already devised by Bak and Sneppen [15]. The lattice sites in their model represent different *species*, each of which is assigned a barrier against *mutation* corresponding to the smallest barrier between local optima on a rugged *fitness* landscape. The species mutate and interact with adjacent species in much the same way that clusters reconfigure and interact with adjacent clusters in our model. The primary difference between the models is that, whereas clusters cannot move higher than e_Γ on their potential energy landscapes, corresponding to the strength of the external impulse, species are subject to no such energetic constraints (there is no such thing as the "conservation of fitness") and move around their fitness landscapes spontaneously. As long as this difference is borne in mind, we can draw upon the plethora of results already accumulated for the evolution model in analysing our model of compaction (for a review, see [16]).

III. COMPARISON TO EXPERIMENTS

We begin by describing the numerical solution of the model for a system comprising of N clusters. The distribution of barrier heights, $Q(b)$, is defined such that a proportion $Q(b)\delta b$ of the clusters have a barrier height in the range b to $b + \delta b$. As the system evolves, $Q(b)$ exhibits two qualitatively different regions, one for large b and one for small b. Large barriers have either not been touched since the simulation began, or (more likely) they have been redrawn from the uniform distribution $P(b)$ as the consequence of an adjacent cluster reconfiguring. As such, $Q(b)$ for large b must also be uniform, except for statistical fluctuations. The situation is more complicated for small barriers since there is now the added possibility of being selected as the minimum of the system. Very small barriers are unlikely to last long and so $Q(b)$ tails off to zero as $b \to 0$. The boundary between these two regions is given by the *gap* function $G(t)$, which is the largest barrier height that has ever been the minimum of the system. Finding the minimum barrier and giving it a new value can be viewed as a flux from the region $b \leq G(t)$ to the region $b > G(t)$. When there are no barriers left in the region $b \leq G(t)$, larger barriers will be selected as the minimum and so $G(t)$ will increase. If there were no interactions, there would only be this

unidirectional flux and $G(t)$ would slowly approach 1 as $t \to \infty$. However, with interactions there is also a flux in the reverse direction, from $b > G(t)$ to $b \leq G(t)$, corresponding to the new values given to the barriers of adjacent clusters. Hence $G(t)$ in fact approaches a constant value $b^* \in (0, 1)$, where b^* is a function of the lattice connectivity and the system size N.

We have not yet considered the effect of the parameter e_Γ. This appears in the equation for δt, the time step between successive reconfiguration events, which also depends on the current value of the minimum barrier (3). It can be seen from (3) that δt becomes singular when the minimum barrier is greater than or equal to e_Γ. If $e_\Gamma > b^*$ then this can never happen, since the minimum fluctuates between 0 and $G(t)$, and $G(t) \to b^*$ as $t \to \infty$. Accordingly the system approaches a statistical steady state in which δt fluctuates around some constant value. By contrast, if $e_\Gamma < b^*$ then it now becomes possible for $G(t)$, and hence also the minimum, to take values close to e_Γ. As it does so, δt will diverge and the system will freeze into a state in which every cluster has a barrier greater than e_Γ and there can be no further reconfigurations. An example of how $G(t)$ depends on e_Γ is given in Fig. 3 for a $40 \times 40 \times 40$ lattice, for which $b^* \approx 0.21$.
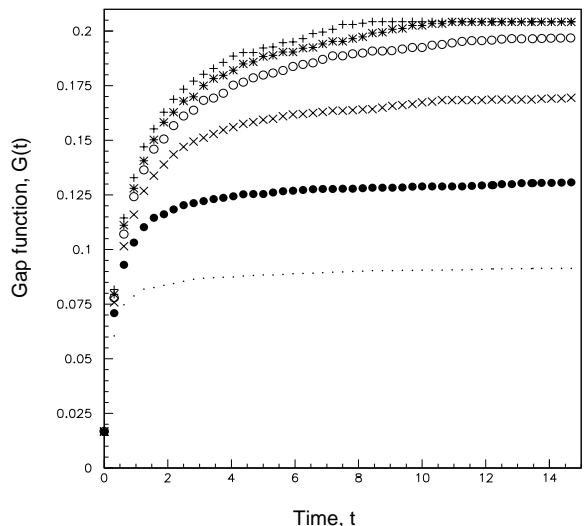

FIG. 3. Plot of the gap function $G(t)$ for various values of e_Γ, for a $40 \times 40 \times 40$ lattice. Key: Plus signs, $e_\Gamma = 0.4$. Asterixes, $e_\Gamma = 0.3$. Open circles, $e_\Gamma = 0.25$. Crosses, $e_\Gamma = 0.2$. Filled circles, $e_\Gamma = 0.15$. Dots, $e_\Gamma = 0.1$. Note that in this and all subsequent plots we have taken the time step to be $\delta t = \exp\{e_\Gamma/(e_\Gamma - b_{\min})\}/N$, where N is the system size, so the units on the time axis are arbitrary.

The model has so far been described in terms of the energy impulse per cluster e_Γ and the barrier distribution $Q(b)$. However, the experimental results were given in terms of an *acceleration* parameter Γ and the *density* ρ. Before comparing the model with the experimental results, we must first consider how these two sets of quantities are related. We start with e_Γ and Γ. The acceleration parameter Γ is defined as the peak acceleration

4

during the perturbation scaled by gravity, $\Gamma = a_{\max}/g$. This was also found to be the relevant parameter for the stability of a bead heap under vibration [17]. Although it seems reasonable that a higher Γ should mean more energy is distributed throughout the system and hence a higher e_Γ, the precise relationship is likely to be very complex and we have been unable to derive a formula relating the two. Instead we simply assume that, for the small vibrations considered here, the relationship is approximately linear, $e_\Gamma \propto \Gamma$.

Trying to quantify the relationship between the barrier distribution and density is more problematic since a potential energy barrier is an intrinsically abstract concept. Nonetheless, a rough formula can be derived as follows. Consider an individual cluster with a barrier b_{clust} and density ρ_{clust}. The cluster's horizontal cross sectional area is assumed to remain roughly constant throughout the compaction process, so the typical vertical separation between the granule centres will be inversely proportional to ρ_{clust}. The cluster cannot reconfigure unless this vertical separation is increased to the order of the granule diameter, thus allowing the granules to move over one another. Since the granule diameter is constant, the change in height required for reconfiguration will also depend inversely upon ρ_{clust}. The potential energy gained by a particle is, of course, proportional to its height increase, so b_{clust} also varies inversely with ρ_{clust}. Extrapolating this result over the entire system amounts to finding the mean barrier height $\bar{b}$, so finally we have

$$\bar{b} \sim \rho^{-1}. \qquad (4)$$

This derivation is simplified in that, for instance, it does not incorporate the effect of adjacent clusters on the value of b_{clust}. We expect it to work for overall trends in density but not for small fluctuations.

We are now in a position to test the model against the experimental results. As mentioned in the introduction, the density was experimentally found to relax inverse logarithmically with time, $\rho(t) \sim (\log t)^{-1}$ [7]. From (4) the corresponding relationship in terms of the mean barrier height is therefore $\bar{b}(t) \sim \log t$, which will show up as a straight line on a graph of $\bar{b}(t)$ vs $\log t$. Such a graph is given in Fig. 4 for a range of values of e_Γ. Linear behaviour is apparent over a broad range of densities for $e_\Gamma > b^*$, confirming logarithmic relaxation towards the statistical steady state. For $e_\Gamma < b^*$, the relaxation is initially logarithmic but slows down as the frozen steady state is approached. Note that although the logarithmic behaviour is robust, the actual values on the axes depend upon which of the various arbitrary choices mentioned in the previous section have been made and hence have no physical meaning.

Little has been said so far about initial conditions. Before the first selection of the minimum barrier $Q(b)$ is uniform over the entire range $[0,1]$, so that even a small e_Γ will cause a significant amount of reconfiguration. This corresponds to a state of *minimum compactivity* which is very difficult to attain experimentally. For

instance, there will always be a certain amount of background noise, and the granules added later to the apparatus will impact upon those already present, inevitably causing some compaction. Instead, the experiments always started from a *slightly* compacted state with a density fraction of 0.577 ± 0.005. This initial compaction can be incorporated into the model by shifting the time axis so that the origin corresponds to when $G(t)$ first becomes greater than a parameter $b_{\mathrm{init}} > 0$. Values of $e_\Gamma \approx b_{\mathrm{init}}$ or less are too small to cause any significant further compaction. This is readily apparent in Fig. 5, where we have plotted $\bar{b}$ in the limit $t \to \infty$ against e_Γ. The line is flat for $e_\Gamma < b_{\mathrm{init}}$, increases linearly for $b_{\mathrm{init}} < e_\Gamma < b^*$ and levels out again for higher e_Γ. This should be compared with the corresponding experimental plot, which is Fig. 3 in [7], from which we estimate that b^* corresponds to $\Gamma \approx 3$.
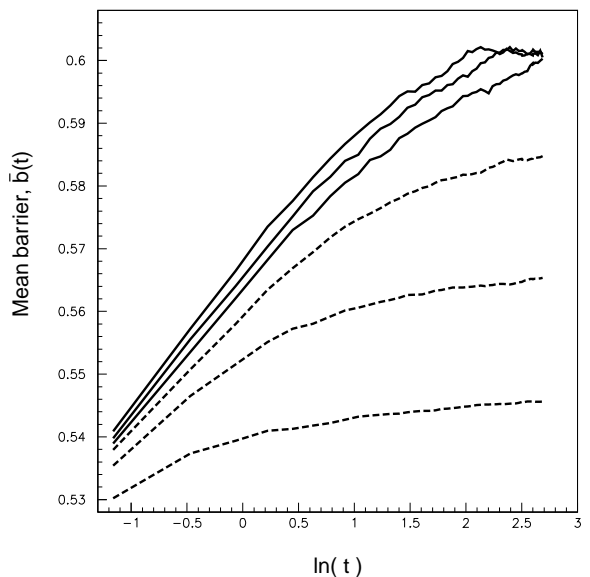

FIG. 4. $\bar{b}(t)$ vs. $\ln t$ for a range of values of e_Γ. The data was taken from single runs on a $40 \times 40 \times 40$ lattice, for which $b^* \approx 0.21$. From top to bottom, the values of e_Γ are: 0.4, 0.3, 0.25, 0.2, 0.15, 0.1. Solid lines have been used for $e_\Gamma > b^*$ and dashed lines have been used for $e_\Gamma < b^*$.

An apparently anomalous feature of Fig. 5 is that the highest densities are to be found, not for large e_Γ, as might be expected, but instead for values of e_Γ near the threshold value b^*. This occurs because of finite size effects. Recall that, for $e_\Gamma > b^*$, the barrier distribution evolves to a state which is uniform for $b > b^*$ with a tail for $b < b^*$. It is the very existence of this tail, which disappears in the thermodynamic limit $N \to \infty$, that reduces the mean barrier $\bar{b}$ for finite systems. When e_Γ is slightly less than b^* then, although the uniform region is slightly broader, the selection process can remove some of the barriers from the tail permanently and so the net effect is to increase $\bar{b}$. An even greater degree of compaction can be obtained if a system with $e_\Gamma > b^*$ is first allowed to self-organise to the statistical steady

state, then e_Γ is *slowly* reduced to zero to remove as much of the tail as possible. Quickly reducing e_Γ will not give enough time for the selection process to work before the system froze and so $\bar{b}$ would barely change. An example of this process is given in Fig. 6, where to accentuate the finite size effects a $4 \times 4 \times 4$ lattice was used. Nowak *et.al.* have produced similar plots from their experiments, which they regard as a type of annealing process [11,18]. They label the lower branch of the graph, when the intensity of vibration is increased for the first time, as "irreversible". In the language of our model, we prefer to call this the *self-organising* branch. The self-organising branch meets an upper *reversible* branch around the point $\Gamma^* \approx 3$. This is to be expected since, as mentioned in the previous paragraph, this value of Γ corresponds to the threshold value b^*, that is, the point at which the system can self-organise into the statistical steady state. According to the model, the change in density along the upper branch is due to the effects of finite size, so there should be a greater variation when larger beads are used in the same sized apparatus. This is in agreement with the experiments except for when the largest bead size was used [18]. In this case, although the overall density variation was the greatest, a disproportionately large amount of it occurred along the self-organising branch, possibly due to the cylinder walls aligning the beads into a highly compact crystalline configuration. Another feature observed in the experiments is that the threshold value Γ^* appears to increase when Γ is updated more rapidly. The model agrees with this and attributes it to the larger number of steps that will take place before the system has had time to self-organise.
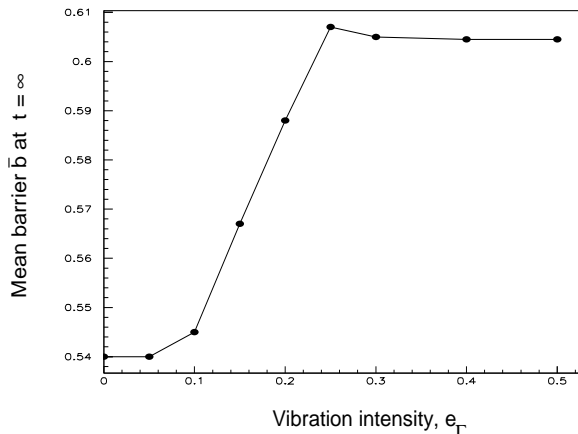

FIG. 5. The mean barrier height $\bar{b}$ in the final steady state as a function of e_Γ. Note that since $\bar{b} \propto (\rho_0 - \rho)^{-1} \sim \rho$ the vertical axis can also be identified as the (approximate) density. The simulations were performed on a $10 \times 10 \times 10$ lattice and averaged over 1000 runs. $b_{\text{init}} = 0.08$ and $b^* \approx 0.25$.

For $e_\Gamma > b^*$ the steady state is statistical in nature, so another test for the model would be to compare the fluctuations of $\bar{b}$ around its steady state value to the fluctuations in density measured experimentally. However, as

previously mentioned, the argument relating $\bar{b}$ to ρ is not expected to hold for small changes. The change in density caused by, say, a single reconfiguration event will be sensitive to the exact positions of a large number of granules at that instant in time. The experimental plot of density fluctuations is Gaussian in form [11], indicative of the large number of independent factors involved. A more revealing distribution is the power spectrum of density fluctuations, $S(f)$, where the frequency f is measured in units of $(\text{taps})^{-1}$. Experimentally, $S(f)$ was found to obey the power law $S(f) \propto f^{-\delta}$, with $\delta = 0.9 \pm 0.2$, for a broad range of f. Apart from finite size effects, the model predicts a power law with $\delta = 1$ [16]. When large intensities of vibration were applied in the experiments, the power law behaviour was broken up by regions with $\delta = 0, 0.5$ or 2. We cannot account for this and attribute it to the expected breakdown of the model for large vibrations.
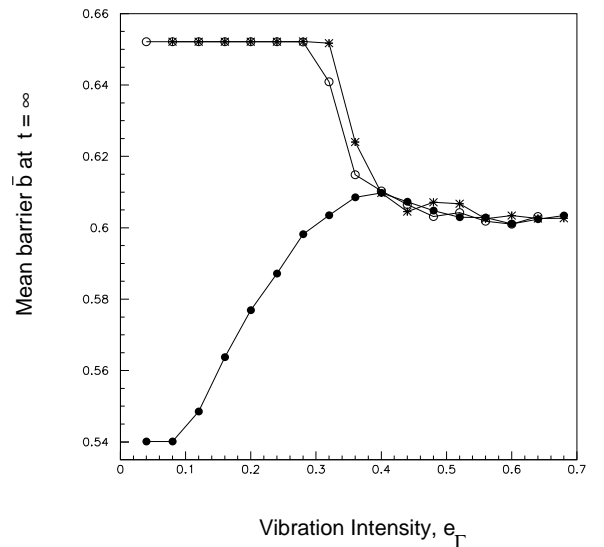

FIG. 6. Annealing curve for a $4 \times 4 \times 4$ lattice, for which $b^* \approx 0.38$. e_Γ first increases from 0.04 to 0.68 in steps of 0.04 (filled circles), then decreases by the same step size from 0.68 to 0.04 (open circles). Finally, e_Γ is increased up to 0.68 again (asterixes). b_{init} was set at 0.08. Each simulation was run until $t \approx 156$, and the final plot was averaged over 1000 such runs.

We end this section by briefly considering how the model might also be applied to a set of related experiments. Jaeger *et.al.* [19] have shown that the angle of repose $\theta(t)$ of granular media in a half-filled cylindrical drum relaxes according to $\theta(t) \sim \log t$ when vibrated. Furthermore, they also demonstrated the existence of a threshold in the intensity of vibration below which the relaxation was qualitatively slower. If we ignore the compaction process which presumably occurs in the bulk of the pile, then the typical vertical separation between granule centres is now proportional to $\tan\theta$, although for the range of angles involved we can use $\tan\theta \approx \theta$ instead. We can now repeat the argument given earlier for density

and find that the relationship between the mean barrier and the slope is $\bar{b} \sim \theta$, to first order. Hence the model also predicts relaxation of the form $\theta(t) \sim \log t$ and the existence of the threshold in the intensity of vibration. However, we have reservations in applying the model to this new geometry since it blatantly involves a global, albeit slow, movement of granules over the surface, something which we have explicitly stated the model does *not* cater for. It should also be mentioned that other theoretical explanations for this behaviour have already been given [4,5,19].

IV. MEAN-FIELD ANALYSIS

The picture presented thus far can be extended by considering a mean field version of the model which is open to quantitative analysis. This simplified model exhibits many of the traits apparent in the exact model, especially in the relaxation towards the statistical steady state. However, it behaves very differently in the steady state itself, and we refer the reader elsewhere for analysis of the original model in this much studied regime [15,16]. The required mean field approximation is to be achieved in two stages. First, all spatial definition is removed. This means that, when the cluster with the smallest barrier in a system of N clusters is found and reconfigured, K other clusters are chosen at random from the remaining $N - 1$ and their barriers given new values. These K clusters are equivalent to the adjacent clusters in the original model, so for example $K = 6$ corresponds to a 3 dimensional system. The second simplification is to assume that N is very large. In this way the system can be described by continuous rather than discrete variables, to within an error margin of $O(1/N)$.

For the first part of this section, the evolution of the system will be described in terms of a time variable τ which increases by $1/N$ between successive reconfigurations. The inclusion of the variable time step given in (3) will be postponed until later. The system is described by the cumulative barrier distribution $C(b, \tau)$, which is defined as the proportion of clusters with barriers less than b at time τ and is related to $Q(b, \tau)$ by

$$C(b, \tau) = \int_0^b Q(x, \tau)\, dx . \qquad (5)$$

The time scale has been normalised to one reconfiguration per cluster per unit τ, so $C(b, \tau)$ evolves according to

$$\frac{\partial C(b, \tau)}{\partial \tau} = -\theta(b - b_{\min}(\tau)) - K\,C(b, \tau) + b\,(K + 1) , \qquad (6)$$

where $b_{\min}(\tau)$ is the value of the minimum barrier in the system at time τ and $\theta(b) = 1$ for $b > 0$ and 0 otherwise. The removal of the minimum barrier has the effect of reducing $C(b, \tau)$ for all values of $b > b_{\min}(\tau)$ but leaves it unchanged for $b < b_{\min}(\tau)$. This is handled by the first term on the right hand side of (6). In a similar manner, the second and third terms account for the selection of the K random nearest neighbours and the $K + 1$ new barrier values, respectively. It is straightforward to check that (6) preserves $C(0, \tau) = 0$, $C(1, \tau) = 1$ and $C(b_1, \tau) \geq C(b_2, \tau)$ for $b_1 > b_2$, for all values of τ.

The rate equation (6) is not yet in a closed form because it involves the unknown quantity $b_{\min}(\tau)$. We might naively try to write down a second equation giving $b_{\min}(\tau)$ in terms of $C(b, \tau)$, perhaps something like $C(b_{\min}(\tau), \tau) = 1/N$. However, it must be recalled that errors of $O(1/N)$ have already been made in going from the discrete model to this continuous description, and so $C(b, \tau)$ cannot be used to this degree of accuracy. Indeed, any attempt to define the minimum barrier within a continuum framework is doomed to failure for this very reason. We are forced to conclude that there can be no set of closed equations in terms of $C(b, \tau)$. All is not lost, however, since this problem can be partially circumnavigated by use of the gap function $G(\tau)$. As before, $G(\tau)$ is defined as the highest value that $b_{\min}(\tau)$ has ever taken, or more formally,

$$G(\tau) = \sup_{0 \leq z \leq \tau} b_{\min}(z) . \qquad (7)$$

Values of b greater than $G(\tau)$ must by definition be greater than every value $b_{\min}$ has taken up to a time τ. This allows for (6) to be simplified to

$$\frac{\partial C(b, \tau)}{\partial \tau} = -(K\,C(b, \tau) + 1) + b\,(K + 1) , \qquad (8)$$

for $b > G(\tau)$. This can be solved by substituting $C(b, \tau) = \alpha(\tau)b + \beta(\tau)$ and comparing coefficients of b. With the initial condition $C(b, 0) = b$ (so $b_{\text{init}} = 0$), the result is

$$C(b, \tau) = b + \frac{b - 1}{K}\left(1 - e^{-K\tau}\right) \qquad (9)$$

The fact that $C(b, \tau)$ is linear means that the barrier distribution $Q(b, \tau)$ is uniform for $b > G(\tau)$, as expected. The solution (9) holds from $b = 1$ down to $b \approx G(\tau)$, where the continuum approximation starts to break down and we have entered into the asymptotic tail. Since there are only $O(1/N)$ clusters in this tail, the value of $G(\tau)$ will correspond to the point at which $C(b, \tau)$ is zero, ie. $C(G(\tau), \tau) = 0$. Together with (9) this allows for the time dependent form of $G(\tau)$ to be found,

$$G(\tau) = \frac{1 - e^{-K\tau}}{K + 1 - e^{-K\tau}} . \qquad (10)$$

Ray and Jan have also found this result by an alternative method [20]. The threshold value of b in this mean field model is therefore

$$b^* = \lim_{\tau \to \infty} G(\tau) = \frac{1}{K+1} \,, \qquad (11)$$

which is smaller than in the exact model.

In this approximation, the mean barrier height $\bar{b}$ behaves in the same way as the gap function. This is because, to $O(1/N)$, there is no tail for $b < G(\tau)$ and the barrier distribution is uniform for $b > G(\tau)$, so $\bar{b}(\tau) = (1 + G(\tau))/2$, which is just a linear rescaling. Hence we expect $G(\tau)$ to vary logarithmically with τ. When the expression for $G(\tau)$ given in (10) is plotted against $\log \tau$ it exhibits a linear region similar to the exact model, but not extending quite as close to the steady state. The gradient of $G(\tau)$ in this log-linear plot is

$$\frac{\mathrm{d}G(\tau)}{\mathrm{d}(\ln \tau)} = \tau \frac{\mathrm{d}G(\tau)}{\mathrm{d}\tau} = \tau G'(\tau) \,. \qquad (12)$$

The linear region occurs around the point where the gradient is stationary, ie. when the second derivative is zero,

$$\frac{\mathrm{d}}{\mathrm{d}(\ln \tau)} \left(\frac{\mathrm{d}G(\tau)}{\mathrm{d}(\ln \tau)} \right) = \tau \left(G'(\tau) + \tau G''(\tau) \right) = 0 \,. \qquad (13)$$

The solution with $\tau = 0$ corresponds to the singularity in $\ln \tau$ and can be ignored. Using (10), the non-trivial solution is

$$\tau = \frac{1}{K} \tanh \frac{K}{2}(\tau + \tau_0) \,, \qquad (14)$$

where the constant $\tau_0 = (\ln(K+1))/K$. Since the slope is roughly constant in this region there is no need to find the exact value of τ that satisfies (14). Instead we observe that, for large K, the tanh function is roughly equal to 1 for all $\tau > 0$, so an approximate solution is $\tau \approx 1/K$ and hence the slope is

$$\left. \frac{\mathrm{d}G(\tau)}{\mathrm{d}(\ln \tau)} \right|_{\tau \approx \frac{1}{K}} \approx \frac{Ke}{[(K+1)e - 1]^2} \,. \qquad (15)$$

We now turn to consider the effect of the variable timestep δt as defined in (3), which depends on $b_{\min}$ and e_Γ. The quantity $b_{\min}$ is unknown, but we know from the discrete model that it fluctuates between 0 and $G(\tau)$ and therefore substituting $G(\tau)$ for $b_{\min}(\tau)$ gives a qualitatively identical solution. The new time scale is denoted by $t(\tau)$ and is defined by

$$\frac{\mathrm{d}t}{\mathrm{d}\tau} = \exp \left\{ \mu \left(\frac{e_\Gamma}{e_\Gamma - G(\tau)} \right) \right\} \,. \qquad (16)$$

For small τ, $G(\tau) = \tau + O(\tau^2)$ and (16) can be solved with the initial condition $t(0) = 0$ to give

$$t(\tau) = e^\mu \left(\tau + \frac{\mu}{2e_\Gamma} \tau^2 + O(\tau^3) \right) \,, \qquad (17)$$

which is linear up to $\tau = O(e_\Gamma^{\frac{1}{2}})$. The behaviour of $t(\tau)$ for large τ depends upon whether e_Γ is greater than,

less than or equal to the threshold value $b^* = \frac{1}{K+1}$. For $e_\Gamma > b^*$, $G(\tau) \to \frac{1}{K+1}$ as $\tau \to \infty$ and consequently

$$t \sim \tau \exp \left\{ \mu \left(\frac{e_\Gamma}{e_\Gamma - \frac{1}{K+1}} \right) \right\} \,. \qquad (18)$$

The time scale is stretched by a constant factor, but otherwise the system approaches the same statistical steady state as before. For $e_\Gamma < b^*$, (16) becomes singular at the point $\tau = \tau_{\mathrm{crit}}$ at which $G(\tau_{\mathrm{crit}}) = e_\Gamma$. Since δt diverges there are no more reconfigurations and the system is in a frozen steady state. The precise nature of this singularity can be found by substituting $\tau = \tau_{\mathrm{crit}} - \epsilon$ into (16), with ϵ small and positive. As $\epsilon \to 0$, $t(\tau)$ diverges according to

$$\left. \frac{\mathrm{d}t}{\mathrm{d}\tau} \right|_{\epsilon \to 0} \sim e^{A/\epsilon} \,, \qquad (19)$$

where the constant

$$A = \mu \frac{e_\Gamma}{(1 - e_\Gamma)(1 - (K+1)e_\Gamma)} \,. \qquad (20)$$

Finally, for $e_\Gamma = b^*$ (16) can be algebraically reduced to

$$\left. \frac{\mathrm{d}t}{\mathrm{d}\tau} \right|_{\tau \to \infty} \sim \exp \left\{ \mu \frac{K+1}{K} e^{K\tau} \right\} \qquad (21)$$

for large τ, which is divergent.

Now that we have confirmed that e_Γ has the same effect in the mean field model as in the exact model, we need to see what it does to the rate of logarithmic decay. This is straightforward for $e_\Gamma \gg b^*$ since

$$t = e^\mu \tau + O(e_\Gamma^{-1}) \,, \qquad (22)$$

so to first order in e_Γ^{-1} the time scale is just stretched by a constant factor, which does not alter the gradient in a log-linear plot. This means that slope of $G(t)$ vs $\log t$ is the same as the slope of $G(\tau)$ vs $\log \tau$ and (15) can be used without modification. For instance, in the exact system with large e_Γ the slope is approximately 0.048 in 3 dimensions, whereas the value predicted by (15) for $K = 6$ is 0.050.

Modifying (15) to incorporate $e_\Gamma < \infty$ is troublesome and we have been unable to derive a general formula. Nonetheless there is still some hint of a correspondence between this analysis and the experiments. In [7] Knight *et.al.* introduce a parameter τ which we call τ_{exp} so as not to confuse it with our τ. τ_{exp} gives a rough measure of the time scale of the relaxation process. We tentatively equate this to the quantity $\mathrm{d}t/\mathrm{d}\tau$, and indeed the experimental plot of τ_{exp} vs Γ looks similar to the form of $\mathrm{d}t/\mathrm{d}\tau$ given in (16). However, this is not a robust feature of the model and so it is impossible to come to any concrete conclusions. The experimental data also shows a noticeable change in behaviour for small Γ. This could be caused the system entering into the frozen

steady state before the logarithmic relaxation has had a chance to take hold, ie. when $\tau_{\text{crit}} \ll \frac{1}{K}$, although it could just be the effect of the initial compaction.

Finally, we demonstrate how this analysis can be extended to incorporate energy dissipated by a reconfiguring cluster to its nearest neighbours. Suppose that each adjacent cluster receives an energy e_{diss} and immediately reconfigures if its barrier is smaller than this, dissipating a further energy e_{diss} to each of its neighbours, and so on. Using the same mean field approximations as before, the net effect of this avalanche between perturbations is to increase the number of barriers that change value at each time step. Of the K random nearest neighbours, Ke_{diss} will immediately reconfigure and so the total number of new barriers per time step $d\tau$ is now

$$K + K(Ke_{\text{diss}}) + K(Ke_{\text{diss}})^2 + K(Ke_{\text{diss}})^3 + \ldots$$

$$= \frac{K}{1 - Ke_{\text{diss}}}\,, \tag{23}$$

for $e_{\text{diss}} < \frac{1}{K}$. Larger values of e_{diss} are unphysical since they result in perpetual reconfiguration. The new rate equation for $C(b,\tau)$ is

$$\frac{\partial C(b,\tau)}{\partial \tau} = -\theta(b - b_{\min}(\tau)) - \frac{K}{1 - Ke_{\text{diss}}}$$

$$+ \left(1 + \frac{K}{1 - Ke_{\text{diss}}}\right) b\,, \tag{24}$$

which can be solved as before to give

$$C(b,\tau) = b + \frac{b-1}{K}(1 - Ke_{\text{diss}}) \left(1 - \exp\left[-\frac{K\tau}{1 - Ke_{\text{diss}}}\right]\right) \tag{25}$$

for $b > G(\tau)$. This is the same as the solution already given in (9) except that K has been replaced by the effective number of random nearest neighbours $K/(1 - Ke_{\text{diss}})$. The time scale is similarly stretched by the constant factor $1 - Ke_{\text{diss}}$. Hence the inclusion of energy dissipation in this manner does not alter the behaviour of the system, nor does it change the slope of $G(\tau)$ in a log-linear graph.

V. SUMMARY AND DISCUSSION

We have presented a theoretical model for the compaction of granular materials by low intensity perturbations which appears to agree well with a range of experimental results. This includes the logarithmic relaxation, the effect of varying the intensity of vibration resulting in a so-called "annealing" curve, and the power spectrum of density fluctuations in the steady state. We have segmented the granular media into local subsystems or clusters which represent ensembles of granules that collectively reconfigure. Associated with each cluster is a potential energy barrier against reconfiguration. Whenever a perturbation gives a cluster enough energy to cross over its barrier into a new configuration, nearby clusters are disrupted and their barriers take on new values. The system behaviour is dominated by this dynamical interaction between clusters and fine detail such as the choice of distribution for the barrier values makes little or no difference. Indeed, it is this very robustness that leads us to hope that the model might correctly describe the mechanism underlying the compaction process, despite its algorithmic simplicity.

It has been suggested that standard statistical mechanics can be applied to granular materials if the fundamental quantities involved are suitably reinterpreted [21,22]. Volume plays the role of energy, and the quantity conjugate to volume is known as *compactivity*, which is the analogue of temperature. The compactivity is infinite when the system is at its maximum volume and zero when it is at its minimum. Our model can also be described in terms of volume rather than energy since the external perturbations increase the volume of the system as well as its energy. Hence we can assign a volume barrier to each cluster which must be exceeded for reconfiguration to take place. In this way, we can see the beginnings of a link to the modified statistical mechanics, perhaps with the barriers being in some way related to the compactivity. This is just speculation, however, and further investigation is required. There are also be many ways in which the model can be enhanced make it more physically realistic. For instance, the model is currently isotropic, but real granular media exhibits a density gradient with the densest regions near the bottom.

There is another way to compact granules into a smaller volume, and that is simply to apply a uniform pressure. This forces the granules to rearrange into a higher density state, as with the perturbation-induced compaction studied in this paper, although the granules are now also subject to deformation and fracturing. A theoretical model for compaction by applied pressure has been proposed which treats the media as being comprised of a number of subsystems, each of which is associated with a pressure barrier [23]. This obviously bears some similarity to the approach we have adopted in constructing our model. A crucial difference is that the subsystems in the pressure model do not interact and the values for the barriers are simply drawn from a suitable distribution. In our model, the choice of distribution is unimportant and it is the dynamical interactions between subsystems that dominates the system behaviour. It would be interesting to see if the interacting cluster picture can be applied to this or any other experimental situation involving granular materials.

*   Electronic address: David.Head@brunel.ac.uk

†   Electronic address: G.J.Rodgers@brunel.ac.uk

[1] H. M. Jaeger and S. R. Nagel, Science **255**, 1523 (1992).

[2] H. M. Jaeger, S. R. Nagel and R. P. Behringer, Rev. Mod. Phys. **68**, 1259 (1996).

[3] P. E. Evans and R. S. Millman in *Perspectives in Powder Metallurgy, Vol 2 : Vibratory Compacting* (Plenum Press, New York, 1967).

[4] Anita Mehta, Physica A **186**, 121 (1992).

[5] Anita Mehta in *Granular Matter: An Interdisciplinary Approach*, edited by Anita Mehta (Springer-Verlag, New York, 1994).

[6] G. C. Barker and Anita Mehta, Phys. Rev. E **47**, 184 (1993).

[7] J. B. Knight, C. G. Fandrich, C. N. Lau, H. M. Jaeger and S. R. Nagel, Phys. Rev. E **51**, 3957 (1995).

[8] S. J. Linz, Phys. Rev. E **54**, 2925 (1996).

[9] E. Ben-Naim, J. B. Knight and E. R. Nowak, *"Slow Relaxation in granular compaction"*, preprint, *cond-mat/9603150*.

[10] P. L. Krapivsky and E. Ben-Naim, J. Chem. Phys. **100**, 6778 (1994).

[11] E. R. Nowak, J. B. Knight, E. Ben-Naim, H. M. Jaeger and S.R. Nagel, *"Density fluctuations in vibrated granular materials"*, to be published in Phys. Rev. E.

[12] T. Boutreux and P. G. de Gennes, *"Compaction of granular materials: a free volume model"*, preprint.

[13] E. Caglioti, V. Loreto, H. J. Herrmann and M. Nicodemi, *"A tetris-like model for the compaction of dry granular media"*, preprint, *cond-mat/9705195*. Submitted to Phys. Rev. Lett.

[14] M. Nicodemi, A. Coniglio and H. J. Herrmann, Phys. Rev. E **55**, 3962 (1997).

[15] P. Bak and K. Sneppen, Phys. Rev. Lett. **71**, 4083 (1993).

[16] M. Paczuski, S. Maslov and P. Bak, Phys. Rev. E **53**, 414 (1996).

[17] P. Evesque and J. Rajchenbach, Phys. Rev. Lett. **62**, 44 (1989).

[18] E. R. Nowak, J. B. Knight, M. Povinelli, H. M. Jaeger and S. R. Nagel, *"Reversibility and irreversibility in the packing of vibrated granular material"*, to be published in Powder Technol.

[19] H. M. Jaeger, C. Liu and S. R. Nagel, Phys. Rev. Lett. **62**, 40 (1989).

[20] T. S. Ray and N. Jan, Phys. Rev. Lett **72**, 4045 (1994).

[21] Anita Mehta and S. F. Edwards, Physica A **157**, 1091 (1989).

[22] S. F. Edwards in *Granular Matter: An Interdisciplinary Approach*, edited by Anita Mehta (Springer-Verlag, New York, 1994).

[23] V. M. Kenkre, M. R. Endicott, S. J. Glass and A. J. Hurd, J. Am. Ceram. Soc. **79**, 3045 (1996).